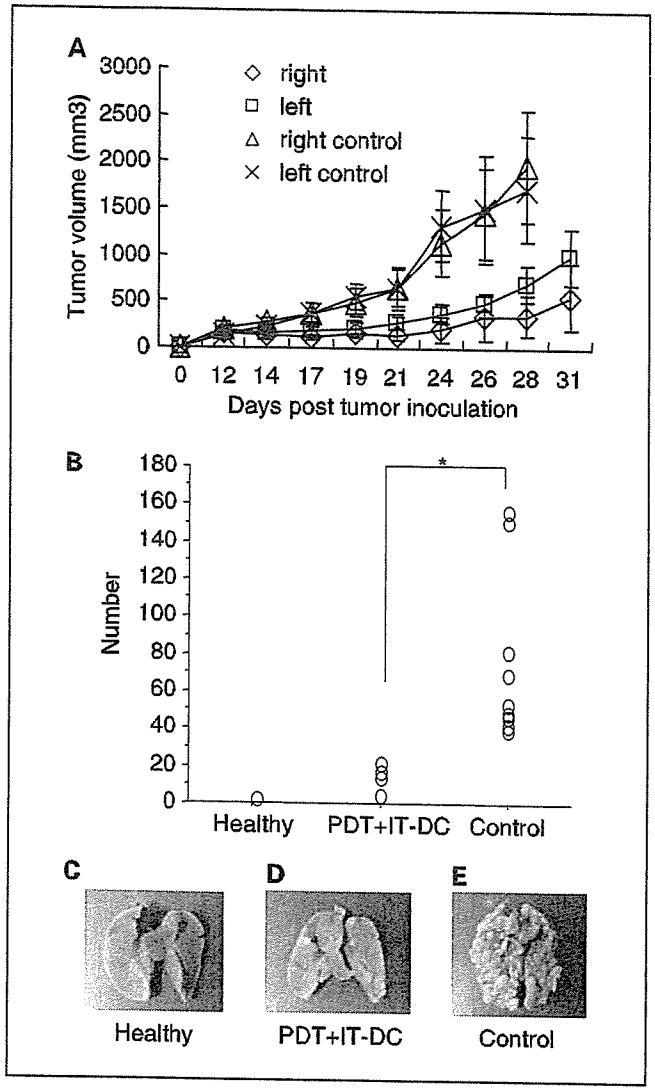

Fig. 6. Systemic tumor-specific immunity induced by local PDT + IT-DC treatment affects tumors at distant sites. *A,* CT26 tumor cells (1×10^6 for each side) were s.c. inoculated in both lower flanks of BALB/c mice. Twelve days later, the tumor-bearing mice were either untreated or treated with PDT + IT-DC into tumors on the right side but not the left side. Tumor growth on the left (untreated) and right (treated) sides was monitored and average tumor volume (±SE) was determined. Shown is the tumor volume on the right (with IT-PBS; △) and left (×) sides of control mice and the right (◇) and left (□) sides of treated mice. Each group contained five mice. *, $P < 0.05$, between left treated and control groups and between right treated and control groups. *B,* 10 BALB/c mice were inoculated s.c. with 1×10^6 CT26 tumor cells on day 0. On day 5, mice were injected i.v. with the same number of CT26 tumor cells, and on day 12, the s.c. tumors were treated with PDT + IT-DC. On day 26, lungs were harvested and stained with Bouin's solution to confirm and quantify lung metastases. *, $P < 0.05$, versus control group. *C,* representative lungs from a healthy mouse. *D,* representative lungs from a tumor-bearing PDT + IT-DC – treated mouse. *E,* representative lungs from an untreated control mouse.

Collectively, these data indicate that PDT + IT-DC therapy induces potent systemic tumor-specific immunity against CT26 colon cancer.

Discussion

One reason postulated for the limited clinical efficacy of most DC-based cancer vaccines studied to date is their variable ability to induce strong antitumor immunity, particularly CTL responses. This variability may have been due to problems related to tumor antigen selection or DC activation. Most DC-based clinical trials have included only a single or few tumor antigens although tumors contain thousands of potential antigens. Moreover, although a wide range of methods have been used to activate DCs and load them with antigens *in vitro*, there is no agreement about which of these methods induces optimal antitumor immunity. We sought to overcome these limitations by introducing unpulsed syngeneic DCs directly into tumors following treatment of the tumors with PDT, which creates a microenvironment that favors tumor antigen acquisition as well as activation of the DCs. The results confirm that PDT-treated tumors contain all of the factors necessary to activate DCs, load them with antigens, and induce an effective systemic antitumor immune response.

Although relatively little work has been done to evaluate the combination of PDT and IT-DC, several previous studies have shown the benefit of combining IT-DC with chemotherapy or radiotherapy (20–26). In contrast to chemotherapy or radiotherapy, PDT is not associated with systemic toxicity. Moreover, PDT renders murine tumors more immunogenic than tumors treated with UV or ionizing irradiation, or frozen and thawed tumors (27). Recently, Jalili et al. (28) reported that PDT in combination with IT-DC had little or no effect on s.c. CT26 tumors but inhibited the growth of contralateral tumors. By contrast, we observed dramatic effects on both local and distant tumors despite the fact that treatment was begun 12 days after inoculation of mice with a higher tumor dose than that studied by Jalili et al. One possible explanation for this surprising result is that we injected the same DC number four times as opposed to twice in their study. Another difference in our two studies is that Jalili et al. used the hematoprophyrin derivative, profimersodium (Photofrin), as a photosensitizer whereas we used ATX-S10 Na(II). Although Photofrin is widely used clinically, its potency is limited by weak absorbance at the shorter range of the red region of the spectrum. In addition, Photofrin is not a pure substance but a mixture of hematoporphyrin monomers, dimers, oligomers, and their dehydration products, and these products are associated with long-lasting skin photosensitivity (12). In contrast, ATX-S10 Na(II) is a homogeneous agent that preferentially accumulates in tumor tissues and is eliminated from normal tissues within 24 to 48 hours after injection. Moreover, its absorption maximum lies at 670 nm, which is longer than that of Photofrin (630 nm) and enables deeper tissue penetration (16). Using ATX-S10 Na(II) as a photosensitizer, we showed that PDT in combination with IT-DC inhibits the growth of two histologically distinct murine tumors. Interestingly, treatment of B16 tumors with combined PDT + IT-DC was at least as effective as it was for CT26, despite the poor immunogenicity of B16 and its well-documented resistance to PDT alone (29).

Our studies clearly show that PDT + IT-DC induces systemic antitumor immunity as well as tumor-specific immunologic memory. In the B16 model, the observation of white hair in untreated sites of mice, of which the tumors had been eradicated following PDT + IT-DC, suggests that treatment induced a systemic immune response against one or more shared antigens present in normal melanocytes as well as B16 tumors. In the CT26 model, PDT + IT-DC treatment of a single s.c. tumor resulted in regression of both contralateral as well as multiple

pulmonary tumors. The cells responsible for mediating tumor regression were cytotoxic T cells as indicated by both *in vitro* cytotoxicty assays and the observation that naïve animals were protected against tumors by adoptively transferred splenocytes from successfully treated tumor-bearing mice. Depletion of specific T-cell subsets (CD4 or CD8) in the adoptively transferred splenocytes indicated the CD8 T cells are the major effector cells induced by the PDT + IT-DC treatment.

Critical to the systemic antitumor effect of PDT + IT-DC is the capture of tumor-associated antigens by DCs as well as DC activation. Whether necrotic or apoptotic tumor cells serve as the superior source of tumor-associated antigens is controversial (30–34). Our data (not shown) strongly suggest that PDT, which induces both apoptosis and necrosis of tumors (12, 28), causes DCs to take up and process tumor antigen released by the dying tumor cells, mature, and become activated *in situ* and then cross-prime T cells against tumor-derived antigens. Interestingly, PDT alone had little or no effect on the growth of B16 tumors and analysis of such tumors following their treatment with PDT revealed a much smaller percentage of apoptotic and necrotic cells than in identically treated CT26 tumors (data not shown). Because PDT + IT-DC was effective as a treatment for both tumors, it seems likely that a relatively small number of dead or dying tumor cells can provide the necessary antigens required for DC-mediated induction of antitumor immunity. Furthermore, because it is known that PDT stimulates the expression of inflammatory cytokines such as tumor necrosis factor α, IL-1, and IL-6 (12, 13), perhaps the presence of such factors in the tumor microenvironment played a critical role in the induction of DC maturation.

In summary, the data presented in this report indicate that PDT + IT-DC results in potent systemic antitumor immunity and regression of tumors including tumors at sites distant from the treated site. Based on these findings, this novel regimen may prove beneficial in the treatment of patients with advanced metastatic disease as well as in the neoadjuvant setting before resection of tumors known to have a high recurrence rate.

Acknowledgments

We thank Claudia Benike, Linda Wu, and Ines Mende for critically reviewing the manuscript.

References

1. Hsu FJ, Benike C, Fagnoni F, et al. Vaccination of patients with B-cell lymphoma using autologous antigen pulsed dendritic cells. Nat Med 1996;2:52–8.
2. Steinman RM, Pope M. Exploiting dendritic cells to improve vaccine efficacy. J Clin Invest 2002;109:1519–26.
3. Banchereau J, Palucka K. Dendritic cells as therapeutic vaccines against cancer. Nat Rev Immunol 2005;5:296–306.
4. Fields RC, Shimizu K, Mule JJ. Murine dendritic cells pulsed with whole tumor lysates mediate potent antitumor immune responses *in vitro* and *in vivo*. Proc Natl Acad Sci U S A 1998;95:9482–7.
5. Song W, Kong HL, Carpenter H, et al. Dendritic cells genetically modified with an adenovirus vector encoding the cDNA for a model antigen induce protective and therapeutic antitumor immunity. J Exp Med 1997;186:1247–56.
6. Boczkowski D, Nair SK, Snyder D, Gilboa E. Dendritic cells pulsed with RNA are potent antigen-presenting cells *in vitro* and *in vivo*. J Exp Med 1996;184:465–72.
7. Condon C, Watkins SC, Celluzzi CM, Thompson K, Falo LD, Jr. DNA-based immunization by *in vivo* transfection of dendritic cells. Nat Med 1996;2:1122–8.
8. Gong J, Chen D, Kashiwaba M, Kufe D. Induction of antitumor activity by immunization with fusions of dendritic and carcinoma cells. Nat Med 1997;3:558–61.
9. Fong L, Engleman EG. Dendritic cells in cancer immunotherapy. Annu Rev Immunol 2000;18:245–73.
10. Engleman EG. Dendritic cell-based cancer immunotherapy. Semin Oncol 2003;30:23–9.
11. Figdor CG, De Vries JM, Lesterhuis WJ, Melief CJM. Dendritic cell immunotherapy: mapping the way. Nat Med 2004;10:475–80.
12. Dougherty TJ, Gomer CJ, Henderson BW, et al. Photodynamic therapy. J Natl Cancer Inst 1998;90:889–905.
13. Gollnick SO, Liu X, Owczarczak B, Musser DA, Henderson BW. Altered expression of interleukin 6 and interleukin 10 as a result of photodynamic therapy *in vivo*. Cancer Res 1997;57:3904–9.
14. Engleman EG, Brody J, Soares L. Using signaling pathways to overcome immune tolerance to tumors. Sci STKE 2004; pe28.
15. Furumoto K, Soares L, Engleman EG, Merad M. Induction of potent antitumor immunity by *in situ* targeting of intratumoral DCs. J Clin Invest 2004;113:774–83.
16. Mori M, Sakata I, Hirano T, et al. Photodynamic therapy for experimental tumors using ATX-S10(Na), a hydrophilic chlorin photosensitizer, and diode laser. Jpn J Cancer Res 2000;91:753–9.
17. Biel MA. Photodynamic therapy and the treatment of head and neck cancers. J Clin Laser Med Surg 1996;14:239–44.
18. Aruga A, Aruga E, Tanigawa K, Bishop DK, Sondak VK, Chang AE. Type 1 versus type 2 cytokine release by Vβ T cell subpopulations determines *in vivo* antitumor reactivity: IL-10 mediates a suppressive role. J Immunol 1997;159:664–73.
19. Barth RJ, Jr., Mule JJ, Spiess PJ, Rosenberg SA. Interferon γ and tumor necrosis factor have a role in tumor regressions mediated by murine CD8+ tumor-infiltrating lymphocytes. J Exp Med 1991;173:647–58.
20. Tong Y, Song W, Crystal RG. Combined intratumoral injection of bone marrow-derived dendritic cells and systemic chemotherapy to treat pre-existing murine tumors. Cancer Res 2001;61:7530–5.
21. Tanaka F, Yamaguchi H, Ohta M, et al. Intratumoral injection of dendritic cells after treatment of anticancer drugs induces tumor-specific antitumor effect *in vivo*. Int J Cancer 2002;101:265–9.
22. Yu B, Kusmartsev S, Cheng F, et al. Effective combination of chemotherapy and dendritic cell administration for the treatment of advanced-stage experimental breast cancer. Clin Cancer Res 2003;9:285–94.
23. Shin JY, Lee SK, Kang CD, et al. Antitumor effect of intratumoral administration of dendritic cell combination with vincristine chemotherapy in a murine fibrosarcoma model. Histol Histopathol 2003;18:435–47.
24. Teitz-Tennenbaum S, Li Q, Rynkiewicz S, et al. Radiotherapy potentiates the therapeutic efficacy of intratumoral dendritic cell administration. Cancer Res 2003;63:8466–75.
25. Ehtesham M, Kabos P, Gutierrez MA, Samoto K, Black KL, Yu JS. Intratumoral dendritic cell vaccination elicits potent tumoricidal immunity against malignant glioma in rats. J Immunother 2003;26:107–16.
26. Song W, Levy R. Therapeutic vaccination against murine lymphoma by intratumoral injection of naive dendritic cells. Cancer Res 2005;65:5958–64.
27. Gollnick SO, Vaughan L, Henderson BW. Generation of effective antitumor vaccines using photodynamic therapy. Cancer Res 2002;62:1604–8.
28. Jalili A, Makowski M, Switaj T, et al. Effective photoimmunotherapy of murine colon carcinoma induced by the combination of photodynamic therapy and dendritic cells. Clin Cancer Res 2004;10:4498–508.
29. Schoenfeld N, Mamet R, Nordenberg Y, Shafran M, Babushkin T, Malik Z. Protoporphyrin biosynthesis in melanoma B16 cells stimulated by 5-aminolevulinic acid and chemical inducers: characterization of photodynamic inactivation. Int J Cancer 1994;56:106–12.
30. Albert ML, Sauter B, Bhardwaj N. Dendritic cells acquire antigen from apoptotic cells and induce class I-restricted CTLs. Nature 1998;392:86–9.
31. Steinman RM, Turley S, Mellman I, Inaba K. The induction of tolerance by dendritic cells that have captured apoptotic cells. J Exp Med 2000;191:411–6.
32. Sauter B, Albert ML, Francisco L, Larsson M, Somersan S, Bhardwaj N. Consequences of cell death: exposure to necrotic tumor cells, but not primary tissue cells or apoptotic cells, induces the maturation of immunostimulatory dendritic cells. J Exp Med 2000;191:423–34.
33. Gallucci S, Lolkema M, Matzinger P. Natural adjuvants: endogenous activators of dendritic cells. Nat Med 1999;5:1249–55.
34. Rovere P, Vallinoto C, Bondanza A, et al. Bystander apoptosis triggers dendritic cell maturation and antigen-presenting function. J Immunol 1998;161:4467–71.

Immunohistochemical Differential Diagnosis Between Large Cell Neuroendocrine Carcinoma and Small Cell Carcinoma by Tissue Microarray Analysis With a Large Antibody Panel

Jun-ichi Nitadori, MD,[1,2,4] Genichiro Ishii, MD,[1] Koji Tsuta, MD,[1] Tomoyuki Yokose, MD,[1] Yukinori Murata, MT,[1] Tetsuro Kodama, MD,[3] Kanji Nagai, MD,[2] Harubumi Kato, MD,[4] and Atsushi Ochiai, MD[1]

Key Words: Lung cancer; Large cell neuroendocrine carcinoma; Small cell carcinoma; Tissue microarray; Immunohistochemistry; Large antibody panel

DOI. 10.1309/DT6BJ698LDX2NGGX

Abstract

To elucidate additional phenotypic differences between large cell neuroendocrine carcinoma (LCNEC) and small cell lung carcinoma (SCLC), we performed tissue microarray (TMA) analysis of surgically resected LCNEC and SCLC specimens. Immunostaining with 48 antibodies was scored based on staining intensity and the percentage of cells that stained positively. Four proteins were identified as significantly expressed in LCNEC as compared with SCLC: cytokeratin (CK)7, 113 vs 49 (P < .0301); CK18, 171 vs 60 (P < .0008); E-cadherin, 77 vs 9 (P < .0073); and β-catenin, 191 vs 120 (P < .0286). Immunostaining of cross-sections containing LCNEC and SCLC components revealed significant expression of CK7, CK18, and β-catenin in the LCNEC component compared with the SCLC component in 2 of 3 cases. Our results indicate that significant expression of CK7, CK18, E-cadherin, and β-catenin is more characteristic of LCNEC than of SCLC, and these findings provide further support that these tumor types are separate entities morphologically and immunophenotypically, if not biologically.

Lung cancer is a major cancer throughout the world and the most common cause of cancer mortality. The revised World Health Organization (WHO) classification of lung cancer published in 1999 classifies neuroendocrine tumors into 4 major histologic categories: low-grade malignant "typical" carcinoid, intermediate-grade malignant "atypical" carcinoid, and 2 high-grade tumors, large cell neuroendocrine carcinoma (LCNEC) and small cell lung carcinoma (SCLC).[1] In 1991, Travis et al[2] introduced the term *large cell neuroendocrine carcinoma* to describe a distinct category of high-grade neuroendocrine tumor with biologic and light microscopic characteristics different from those of high-grade SCLC. Morphologically, LCNEC is characterized by neuroendocrine morphologic features (rosette formation), large tumor cells (3 times larger in diameter than a small resting lymphocyte) with a low nuclear/cytoplasmic ratio, numerous nucleoli, a high mitotic rate (>10 in 10 high-power fields), a large degree of necrosis, and immunohistochemically staining positive for one or more neuroendocrine markers.

Some authors have reported that LCNEC has a poorer prognosis than SCLC,[3,4] whereas others have reported finding no significant difference in outcome between LCNEC and SCLC.[5-7] SCLC is sensitive to chemotherapy, but the optimal therapy for LCNEC has yet to be defined. Demetri et al[8] advocated that LCNEC be treated in a manner similar to SCLC but acknowledged that there may be a greater role for surgical resection in LCNEC. Nevertheless, it remains unclear how patients with LCNEC should be treated. Until now, few investigators have attempted to identify differences in molecular expression between LCNEC and SCLC. Sturm et al[9] reported a significantly higher frequency of thyroid transcription factor (TTF)-1 positivity with SCLCs, but no other biologic markers

with significantly different expression between LCNEC and SCLC have been reported.

Tissue microarray (TMA) analysis is becoming broadly accepted as an efficient and expeditious method in the field of proteomics,[10-12] and it provides a great deal of information that is equivalent to the information obtained from many tissue sections obtained from a large number of patients. It also is suitable for high-throughput molecular profiling of tumor specimens. In the present study, we used TMA with a large panel of antibodies to identify the phenotypic differences between LCNEC and SCLC.

Materials and Methods

Case Selection

During the period from January 1992 to December 2003, a total of 1,921 patients with primary lung carcinoma were treated at the National Cancer Center Hospital East, Chiba, Japan. All primary lung cancers with a pathologic diagnosis based on the classification schema of the third edition of the WHO classification[1] were reviewed, and 49 cases were diagnosed as LCNEC (2.6%). The 10 cases for which an adequate tissue specimen was not available for pathologic review were excluded from the study, leaving a total of 39 cases (2.0%) of LCNEC. TMA also was performed on specimens from 14 cases histologically diagnosed as pure SCLC (0.7%). In addition, 3 cases of SCLC combined with LCNEC were used to verify the results obtained by TMA.

Pathologic Studies

The specimens were fixed with 10% formalin and embedded in paraffin. Serial 4-μm sections were stained with H&E by the alcian blue–periodic acid–Schiff method for cytoplasmic mucin production and by the elastic van Gieson method for elastic fibers. Sections were reviewed by 3 pulmonary pathologists (J.N., G.J., and T.Y.) according to the histologic criteria described in the WHO classification criteria, and discrepancies were resolved by joint discussion of the slides viewed with a multiheaded microscope.

Construction of Tumor TMAs

The most representative tumor areas were selected carefully and marked on the H&E-stained slide for construction of microarrays. TMAs were assembled with a tissue-arraying instrument (Beecher Instruments, Silver Spring, MD).[10] The microarray system consists of thin-walled stainless steel needles approximately 2 mm in diameter and a stylet for transferring and removing the contents of the needle. The assembly is held in an x-y position guide that is manually adjusted with digital micrometers. Core samples are retrieved from selected regions of donor tissue and precisely arrayed in a new (recipient) paraffin block. Extra samples of the specimens were obtained routinely by collecting 2 replicate core samples of tumor in different areas. Specimens from the 39 cases of LCNEC **Image 1B** and **Image 1D** and 14 cases of SCLC **Image 1C** and **Image 1E** were punched, and core samples were mounted in the same donor blocks **Image 1A**.

Normal Control TMA

The normal control TMA was used as the positive control array for each staining. This slide was composed of esophagus, stomach, small intestine, large intestine, liver, pancreas, spleen, brain, heart, lung, skin, testis, kidney, prostate gland, breast, thyroid gland, and adrenal gland samples.

Antibodies and Immunohistochemical Staining

The 48 antibodies used in the study are listed in **Table 1**. Immunohistochemical staining was performed as follows: TMA donor blocks were cut into 4-μm sections and mounted on silane-coated slides. The sections were deparaffinized in xylene and dehydrated in a graded alcohol series, and endogenous peroxidase was blocked with 3% hydrogen peroxide in absolute methyl alcohol. Heat-induced epitope retrieval was performed for 20 minutes at 95°C with a 0.02-mol/L concentration of citrate buffer (pH 6.0). After the slides cooled at room temperature for 60 minutes, they were rinsed with deionized water and incubated overnight with primary antibodies. The slides then were washed 3 times with phosphate-buffered saline and incubated with the EnVision+ System-HRP (DAKO, Glostrup, Denmark). The reaction products were stained with diaminobenzidine and counterstained with hematoxylin. Some antibodies (Table 1) were used in an automated immunostainer (Ventana Medical Systems, Tucson, AZ) after antigen retrieval by microwave heating and citrate buffer.[13]

Identification of Positive Cases

The cases were evaluated in random order without knowledge of patient history. Each case in which more than 10% of the cancer cells reacted positively for an antibody were recorded as positive.

Calculation of Staining Scores

Immunostaining was scored based on the intensity of staining and the percentage of cells that stained positively. Whenever there was a disagreement, the slides were reviewed, and consensus was reached. Staining scores were calculated by multiplying the percentage of positive tumor cells per section (0% to 100%) by the immunohistochemical staining intensity. The sections were classified according to staining intensity as negative (total absence of staining), 1+ (weak staining), 2+ (moderate staining), or 3+ (strong staining), and the scores obtained ranged from 0 to 300. The staining scores obtained for 2 samples from the same specimen were calculated, and the result was recorded as the

DOI: 10.1309/DT6BJ698LDX2NGGX

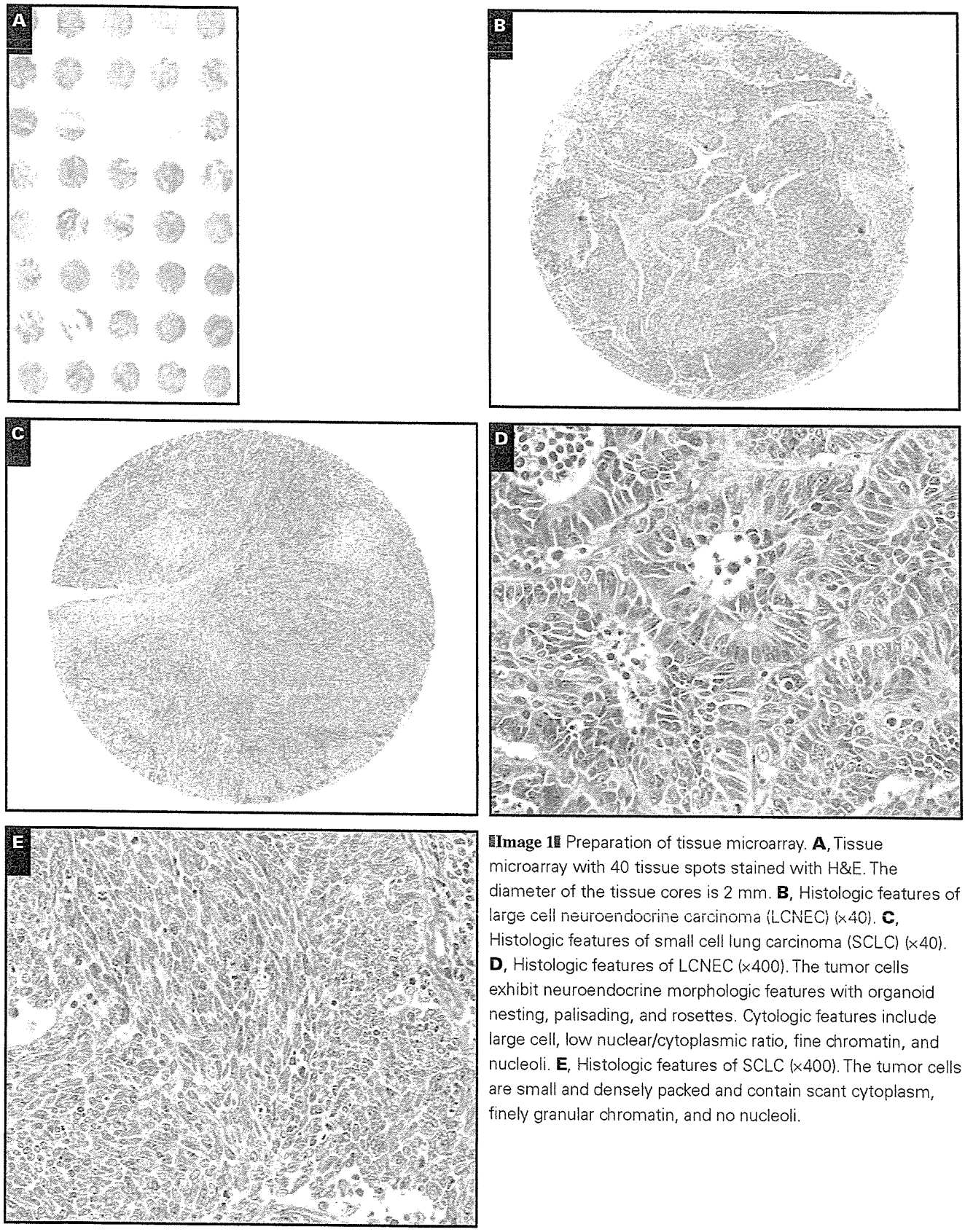

Image 1 Preparation of tissue microarray. **A**, Tissue microarray with 40 tissue spots stained with H&E. The diameter of the tissue cores is 2 mm. **B**, Histologic features of large cell neuroendocrine carcinoma (LCNEC) (×40). **C**, Histologic features of small cell lung carcinoma (SCLC) (×40). **D**, Histologic features of LCNEC (×400). The tumor cells exhibit neuroendocrine morphologic features with organoid nesting, palisading, and rosettes. Cytologic features include large cell, low nuclear/cytoplasmic ratio, fine chromatin, and nucleoli. **E**, Histologic features of SCLC (×400). The tumor cells are small and densely packed and contain scant cytoplasm, finely granular chromatin, and no nucleoli.

DOI: 10.1309/DT6BJ698LDX2NGGX

Table 1
Antibodies Used

Classification/Antibody	Clone	Pretreatment	Dilution	Source
Cytokeratins				
CK1	34βB4	Microwave	1:20	Novocastra, Newcastle upon Tyne, England
CK4	6B10	Microwave	1:100	Novocastra
CK5/6	D5/16 B4	Microwave	1:50	DakoCytomation, Carpinteria, CA
CK7	OV-TL 12/30	Microwave	1:50	DakoCytomation
CK8	35βH11	Microwave	1:25	DakoCytomation
CK10	DE-K10	Microwave	1:50	DakoCytomation
CK13	KS-1A3	Microwave	1:100	Novocastra
CK14	LL002	Microwave	1:20	Novocastra
CK15	LHK15	Microwave	1:40	Novocastra
CK17	E3	Microwave	1:20	DakoCytomation
CK18	DC10	Microwave	1:25	DakoCytomation
CK19	RCK108	Microwave	1:50	DakoCytomation
CK20	Ks20.8	Microwave	1:25	DakoCytomation
Cytoskeletal filaments and markers				
Desmin	DE-R-11	Microwave	Prediluted	Ventana Medical Systems, Tucson, AZ
S-100	Polyclonal	None	Prediluted	Ventana Medical Systems
EMA	Mc5	None	Prediluted	Ventana Medical Systems
Vimentin	3B4	Microwave	Prediluted	Ventana Medical Systems
Drug resistant gene products and related markers				
Pgp	JSB-1	Microwave	1:20	Novocastra
MRP-1	MRPm6	Microwave	1:50	Sanbio, Uden, the Netherlands
MRP-2	M2III-6	Microwave	1:20	Sanbio
BCRP	BXP21	Microwave	1:20	Sanbio
Cox-1	Polyclonal	Microwave	1:50	IBL, Gunma, Japan
Cox-2	Polyclonal	Microwave	1:50	IBL
Apoptosis-associated proteins				
bcl-2	124	Microwave	1:40	DakoCytomation
bcl-x	Polyclonal	Microwave	1:500	Becton Dickinson Biosciences, San Jose, CA
bax	Polyclonal	Microwave	1:20	Oncogene Research Products, Cambridge, MA
bcl-1	P2D11F11	Microwave	Prediluted	Ventana Medical Systems
p 53	DO-7	Microwave	1:50	DakoCytomation
Growth factors and hormone receptors				
EGFR	EGFR.113	Microwave	1:10	Novocastra
c-erbB-2	CB11	Microwave	Prediluted	Ventana Medical Systems
IGFR	24-31	Microwave	1:100	Chemicon, Temecula, CA
c-kit	Polyclonal	Microwave	1:50	DakoCytomation
PgR	1A6	Microwave	Prediluted	Ventana Medical Systems
ER	6F11	Microwave	Prediluted	Ventana Medical Systems
Cellular adhesion molecules				
β-catenin	14	Microwave	1:200	Becton Dickinson Biosciences
E-cadherin	36	Microwave	1:100	Becton Dickinson Biosciences
NCAM	NCC-Lu-243	Microwave	1:25	Nippon Kayaku, Tokyo, Japan
CD29	7F10	Microwave	1:20	Novocastra
CD44	DF1485	Microwave	1:40	Novocastra
Cluster differential markers				
CD15	BY87	Microwave	Prediluted	Ventana Medical Systems
CD30	1G12	Microwave	Prediluted	Ventana Medical Systems
Mucin-related proteins				
Muc-1	Ma695	Microwave	1:100	Novocastra
Muc-2	Ccp58	Microwave	1:100	Novocastra
Muc-5AC	CLH2	Microwave	1:50	Novocastra
Muc-6	CLH5	Microwave	1:50	Novocastra
M-CCMC-1	HIK1083	Microwave	1:10	Kanto Chemical, Tokyo, Japan
Pneumocyte differential markers				
TTF-1	8G7G3/1	Microwave	1:50	DakoCytomation
SPPB	19H7	Microwave	1:25	Novocastra

BCRP, breast cancer resistance protein; EGFR, epidermal growth factor receptor; EMA, epithelial membrane antigen; ER, estrogen receptor; IGFR, insulin-like growth factor receptor; MRP, multidrug resistance protein; NCAM, neural cell adhesion molecule; PgP, P-glycoprotein; PgR, progesterone receptor; SPPB, surfactant precursor protein B; TTF, thyroid transcription factor.

score for that case. If one sample was lost, the staining score was calculated from the data for the remaining specimen alone. The staining scores for the specimens that contained SCLC combined with LCNEC were calculated using the intensity of staining and the percentage of each component stained on the entire slide.

Statistical Analysis

The staining score data are reported as means plus 95% confidence intervals. The Mann-Whitney U test was used to compare the staining scores of the LCNEC group and the SCLC group. All P values reported are 2-sided, and the significance

DOI: 10.1309/DT6BJ698LDX2NGGX

level was set at less than .05. Differences between proportions were evaluated by using the Fisher exact test. All analyses were performed using Statview software (version 5.0 for Windows, SAS Institute, Cary, NC).

Results

Of the 5,406 core samples, 70 (1.3%) were lost on the TMA during processing of the slides for H&E preparation and immunostaining.

Positive Rates of LCNEC and SCLC

The percentages of LCNEC cases and SCLC cases that reacted positively for each antibody are summarized in **Table 2**. A positive reaction for cytokeratin (CK)18 was observed in 38 (97%) of 39 cases of LCNEC and 10 (71%) of 14 cases of SCLC, and the difference was significant ($P = .0143$). A positive reaction for E-cadherin was observed in 30 (77%) of 39 cases of LCNEC and 6 (43%) of 14 cases of SCLC, and the difference was significant ($P = .0419$).

Staining Scores for LCNEC and SCLC

The LCNEC and SCLC staining scores for each antibody are summarized in Table 2. Of the 13 cytokeratins tested, CK7 and CK18 had significantly higher staining scores in LCNEC. CK7 immunoreactivity was found in 30 (77%) of 39 cases of LCNEC and 7 (50%) of 14 cases of SCLC. The average staining score was 113 in LCNEC and 49 in SCLC; the difference was significant ($P = .0301$). **Image 2A** shows CK7 immunostaining of an LCNEC case with a staining score of 270. **Image 2B** shows CK7 immunostaining of an SCLC case with a staining score of 10. The average CK18 staining score was 171 in LCNEC and 60 in SCLC, and the difference was significant ($P = .0008$). **Image 2C** and **Image 2D** show CK18 immunostaining of an LCNEC case with a staining score of 240 and an SCLC case with a staining score of 40. No significant differences between LCNEC and SCLC were found in the expression of the other cytokeratins tested.

LCNEC had significantly higher staining scores for E-cadherin and β-catenin. E-cadherin expression was localized mainly on the membranes of the tumor cells. In some cases, E-cadherin expression was localized in the cytoplasm and nucleus, but results were recorded as negative. The average staining score for E-cadherin was 77 in LCNEC and 9 in SCLC. **Image 2E** and **Image 2F** show that the E-cadherin staining score was 80 in LCNEC and 10 in SCLC. Image 2F shows an E-cadherin staining score of 10 in SCLC. The expression of β-catenin was localized on the membranes and, in some cases, on the nucleus of the tumor cells. We classified the pattern of expression of β-catenin according to whether there was membranous or nuclear staining. Membranous β-catenin staining was found in 38 (97%) of 39 LCNEC cases and all 14 SCLC cases (100%). The average membranous β-catenin staining score was 191 in LCNEC and 120 in SCLC. **Image 2G** shows a membranous β-catenin staining score of 200 in LCNEC. **Image 2H** shows that the β-catenin staining score was 60 in SCLC. Nuclear β-catenin immunoreactivity was found in 5 (13%) of 39 LCNEC cases but in 0 (0%) of 14 SCLC cases. The average nuclear β-catenin staining score was 31 in LCNEC and 0 in SCLC, and the difference was not significant ($P = .4801$). There were no significant differences between LCNEC and SCLC in expression of the other cellular adhesion molecules.

We evaluated the expression of several other biologic markers, but no differences in expression were found between LCNEC and SCLC (Table 2).

Immunohistochemical Staining of CK7, CK18, E-Cadherin, and β-Catenin in Cross-Sections Containing LCNEC and SCLC Components

To determine whether the differences in expression of CK7, CK18, E-cadherin, and β-catenin in LCNEC and SCLC found as a result of the TMA analysis could be applied generally, their expression was evaluated in 3 cases of combined SCLC and LCNEC on slides that contained both components. The staining scores in these 3 cases are summarized in **Table 3**. In cases 1 and 2, expression of CK7, CK18, and β-catenin was clearly higher in the LCNEC components **Image 3**, and the results for these antibodies seemed similar to the results of TMA; however, E-cadherin expression was modestly higher in the LCNEC component in 1 case (case 1).

Discussion

The aim of the present study was to identify the distinct immunophenotypes of LCNEC and SCLC, and the technique used was based on large-scale analysis of protein expression detected by immunohistochemical analysis. Although it must be kept in mind that a potential limitation of TMA is that small core samples might not be representative of whole tumors, particularly in heterogeneous cancers,[14] the use of TMA has the advantage of enabling protein profiling, which probably more closely reflects the biologic characteristics of the tumor cells than does RNA detection. In the present study, we used the products of the staining intensity and distribution scores to assess immunoreactivity because they reveal phenotypic differences in greater detail. The TMA method identified 4 proteins as being overexpressed in LCNEC compared with SCLC: CK7 and CK18, which are involved in cytoskeleton organization, and β-catenin and E-cadherin, which are involved in cell adhesion. The results obtained were not surprising because the most striking morphologic differences between LCNEC and SCLC are cell shape and adhesiveness.

DOI: 10.1309/DT6BJ698LDX2NGGX

Table 2
Positivity Rate, Staining Scores, and *P* Values for 39 Cases of LCNEC and 14 Cases of SCLS

Classification/Antibody	Positive Cases*			Staining Score		
	LCNEC	SCLC	*P*	LCNEC	SCLC	*P*
Cytokeratins						
CK1	1 (3)	0 (0)	.9999	0.1	0	.8877
CK4	9 (23)	2 (14)	.7062	2	0.5	.579
CK5/6	5 (13)	0 (0)	.3089	13	0	.4801
CK7	30 (77)	7 (50)	.9	113	49	.0301
CK8	26 (67)	8 (57)	.5238	51	39	.6211
CK10	0 (0)	0 (0)	.9999	0	0	.9999
CK13	4 (10)	2 (14)	.6489	0.5	1.8	.7699
CK14	1 (3)	1 (7)	.4623	0.2	0.4	.8087
CK15	0 (0)	0 (0)	.9999	0	0	.9999
CK17	6 (15)	0 (0)	.178	6.7	0	.3968
CK18	38 (97)	10 (71)	.0143	171	60	.0008
CK19	23 (59)	9 (64)	.7274	20	18	.9517
CK20	1 (3)	1 (7)	.4623	0.3	0.4	.9517
Cytoskeletal filaments and markers						
Desmin	0 (0)	0 (0)	.9999	0	0	.9999
S-100	8 (21)	6 (43)	.157	12	14	.3131
EMA	23 (59)	6 (43)	.2987	61	31	.2379
Vimentin	9 (23)	1 (7)	.2583	4	1	.3329
Drug-resistant gene products and related markers						
Pgp	0 (0)	1 (7)	.2642	0	1	.694
MRP-1	16 (41)	5 (36)	.7274	10	41	.9277
MRP-2	6 (15)	1 (7)	.6601	3	3.9	.6792
BCRP	24 (62)	9 (64)	.8557	39	23	.5056
Cox-1	0 (0)	0 (0)	.9999	0	0	.9999
Cox-2	0 (0)	0 (0)	.9999	0	0	.9999
Apoptosis-associated proteins						
bcl-2	30 (77)	13 (93)	.2583	118	107	.992
bcl-x	38 (97)	14 (100)	.9999	86	93	.364
bax	0 (0)	0 (0)	.9999	0	0	.9999
bcl-1	0 (0)	0 (0)	.9999	0	0	.9999
p53	30 (77)	8 (57)	.1819	170	120	.1609
Growth factors and hormone receptors						
EGFR	9 (23)	2 (14)	.7062	17	24	.4273
c-erbB-2	2 (5)	1 (7)	.9999	11	1	.9277
IGFR	25 (64)	6 (43)	.1664	32	12	.0845
c-kit	28 (72)	10 (71)	.9999	73	98	.6069
PgR	0 (0)	0 (0)	.9999	0	0	.9999
ER	0 (0)	0 (0)	.9999	0	0	.9999
Cellular adhesion molecules						
β-catenin						
Membranous	38 (97)	14 (100)	.9999	191	120	.0286
Nuclear	5 (13)	0 (0)	.3089	31	0	.4801
E-cadherin	30 (77)	6 (43)	.0419	77	9	.0073
NCAM	38 (97)	14 (100)	.9999	174	210	.1576
CD29	35 (90)	14 (100)	.5631	95	79	.9839
CD44	24 (62)	5 (36)	.0959	67	48	.2502
Cluster differential markers						
CD15	16 (41)	5 (36)	.7274	39	19	.709
CD30	0 (0)	0 (0)	.9999	2	0	.8877
Mucin-related proteins						
Muc-1	19 (49)	7 (50)	.9344	39	27	.8957
Muc-2	0 (0)	0 (0)	.9999	0	0	.9999
Muc-5AC	3 (8)	0 (0)	.5572	1.3	0	.6718
Muc-6	5 (13)	3 (21)	.4221	9	4	.7015
M-CCMC-1	0 (0)	0 (0)	.9999	0	0	.9999
Pneumocyte differential markers						
TTF-1	9 (23)	6 (43)	.1819	38	37	.4373
SPPB	5 (13)	2 (14)	.9999	21	1	.9839

BCRP, breast cancer resistance protein; EGFR, epidermal growth factor receptor; EMA, epithelial membrane antigen; ER, estrogen receptor; IGFR, insulin-like growth factor receptor; MRP, multidrug resistance protein; NCAM, neural cell adhesion molecule; PgP, P-glycoprotein; PgR, progesterone receptor; SPPB, surfactant precursor protein B; TTF, thyroid transcription factor.
* Data are given as number (percentage).

DOI: 10.1309/DT6BJ698LDX2NGGX

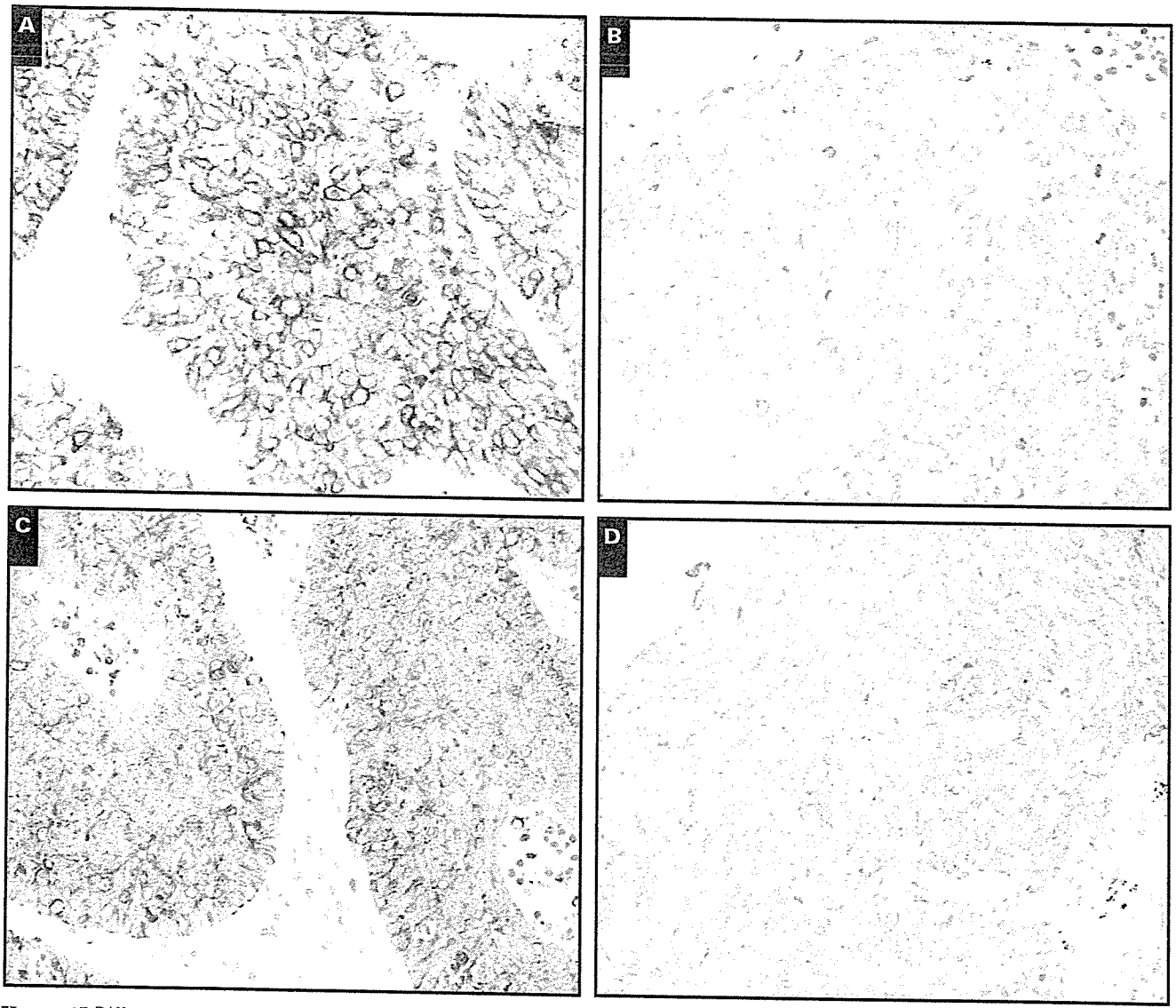

Image 2 Differences in immunostaining of cytokeratin (CK)7, CK18, E-cadherin, and β-catenin between large cell neuroendocrine carcinoma (LCNEC) and small cell lung carcinoma (SCLC). **A**, CK7 immunostaining in LCNEC showing a staining score of 270 (positive cells, 90%; staining intensity, 3+) (×400). **B**, CK7 immunostaining in SCLC showing a staining score of 10 (positive cells, 10%; staining intensity, 1+) (×400). **C**, CK18 immunostaining in LCNEC showing a staining score of 240 (positive cells, 80%; staining intensity, 3+) (×400). **D**, CK18 immunostaining in SCLC showing a staining score of 40 (positive cells, 40%; staining intensity, 1+) (×400).

To our knowledge, this is the first study to identify significant differences in cytokeratin expression between LCNEC and SCLC. In normal adult lung tissue, CK7 and CK18 have been identified primarily in type II alveolar pneumocytes and in bronchial and bronchiolar epithelium. The results of testing for CK7 immunoreactivity in SCLC and LCNEC in previous studies yielded a wide variety of results. Lyda and Weiss[15] demonstrated immunoreactivity for CK7 in 2 (33%) of 6 cases of LCNEC and 2 (5%) of 38 cases of SCLC. By contrast, other studies of SCLC have reported CK7 expression in 4 (40%) of 10 cases,[16] 4 (80%) of 5 cases,[17] and 1 (9%) of 11 cases.[18] Wetzels et al[19] reported CK18 immunoreactivity in SCLC in 5 (83%) of 6 cases, and another study reported positivity in 8 (80%) of 10 cases.[16] However, CK18 expression had not been determined in LCNEC. The reasons for the discrepancies were unclear, but it should be kept in mind that the articles[16,18,19] were published before LCNEC had been defined and that LCNEC had been lumped together within SCLC in these studies. Most of the cases of LCNEC in our study showed diffuse, strong expression of CK7 and CK18, as opposed to focal and weak expression in SCLC, and significantly increased expression of CK7 (P = .0301) and CK18 (P = .0008) was observed in LCNEC.

DOI: 10.1309/DT6BJ698LDX2NGGX

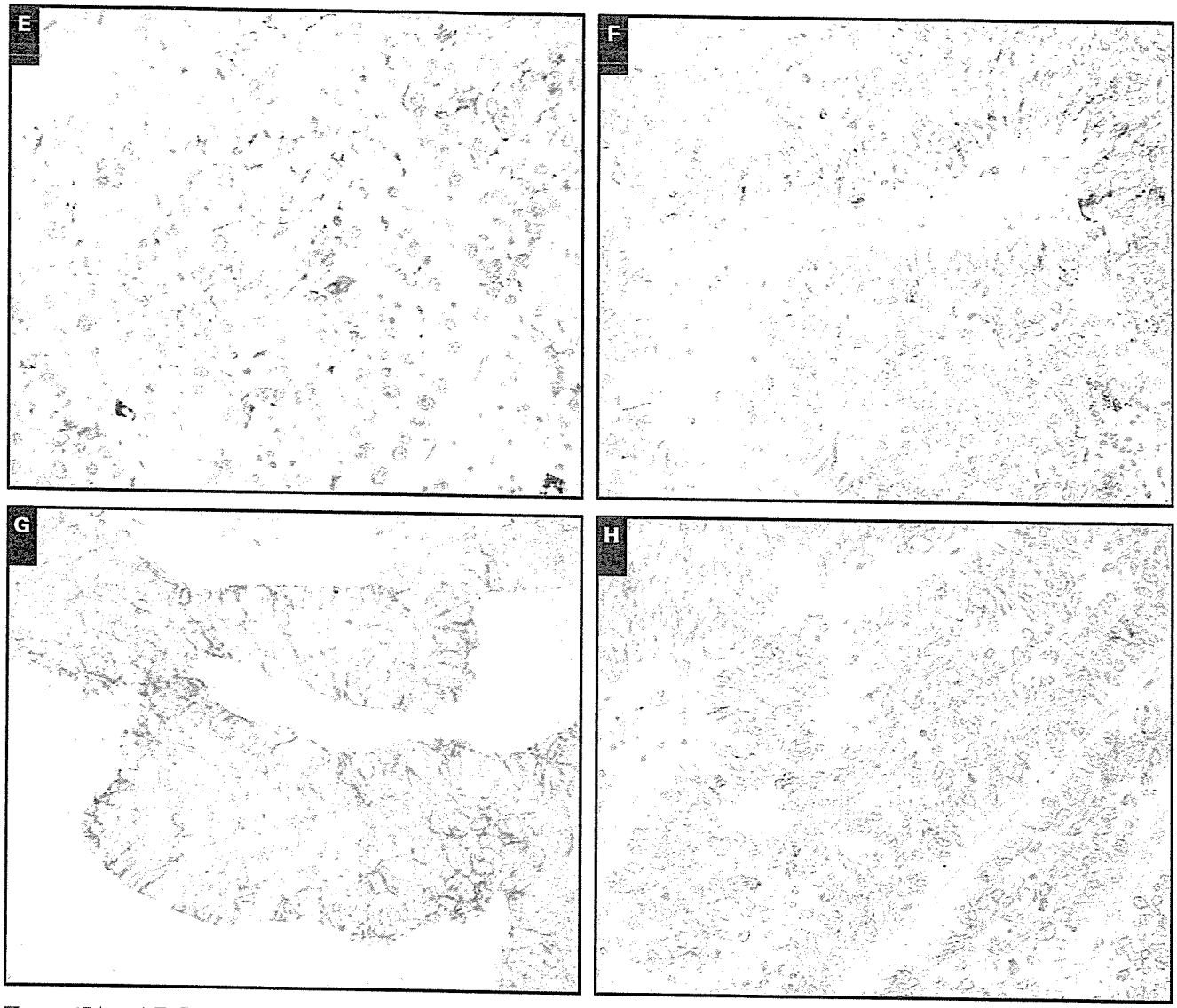

Image 2 (cont) **E**, E-cadherin immunostaining in LCNEC showing a staining score of 80 (positive cells, 80%; staining intensity, 1+) (×400). **F**, E-cadherin immunostaining in SCLC showing a staining score of 10 (positive cells, 10%; staining intensity, 1+) (×400). **G**, Membranous β-catenin immunostaining in LCNEC showing a staining score of 200 (positive cells, 100%; staining intensity, 2+) (×400). **H**, Membranous β-catenin immunostaining in SCLC showing a staining score of 60 (positive cells, 60%; staining intensity, 1+) (×400).

In normal adult lung tissue, E-cadherin and membranous β-catenin staining has been identified in bronchial and bronchiolar epithelium, but no nuclear β-catenin staining has been detected. In the study by Clavel et al,[20] E-cadherin–positive immunoreactivity was observed in 11 (73%) of 15 cases of LCNEC and membranous and nuclear β-catenin immunoreactivity was observed in 14 cases (93%) and 7 cases (47%), respectively, of LCNEC. Rodriguez-Salas et al[21] examined β-catenin expression in 50 pretreatment biopsy specimens of SCLC and reported that 14 (28%) of 50 cases were positive. The results of our own study showed E-cadherin and β-catenin expression in 77% and 97%, respectively, of the LCNEC cases and in 43% and 100%, respectively, of the SCLC cases.

Table 3
Staining Score of SCLC Cases Combined With LCNEC Cases

Case No./ Component	Staining Score			
	Cytokeratin 7	Cytokeratin 18	E-Cadherin	β-Catenin
1				
LCNEC	200	220	50	130
SCLC	10	10	0	20
2				
LCNEC	190	240	40	230
SCLC	10	10	50	60
3				
LCNEC	10	300	100	250
SCLC	0	300	100	240

LCNEC, large cell neuroendocrine carcinoma; SCLC, small cell lung carcinoma.

DOI: 10.1309/DT6BJ698LDX2NGGX

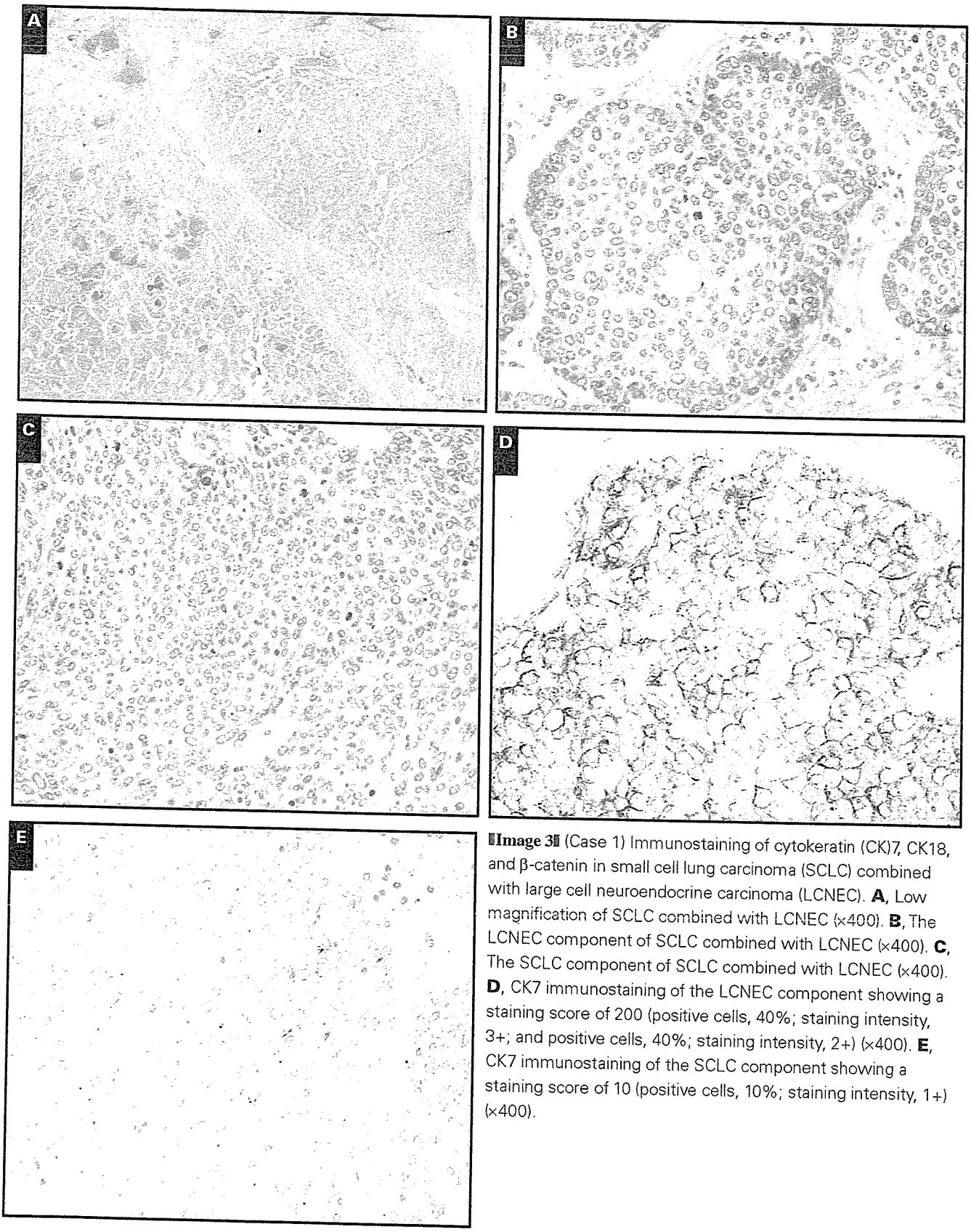

Image 3 (Case 1) Immunostaining of cytokeratin (CK)7, CK18, and β-catenin in small cell lung carcinoma (SCLC) combined with large cell neuroendocrine carcinoma (LCNEC). **A**, Low magnification of SCLC combined with LCNEC (×400). **B**, The LCNEC component of SCLC combined with LCNEC (×400). **C**, The SCLC component of SCLC combined with LCNEC (×400). **D**, CK7 immunostaining of the LCNEC component showing a staining score of 200 (positive cells, 40%; staining intensity, 3+; and positive cells, 40%; staining intensity, 2+) (×400). **E**, CK7 immunostaining of the SCLC component showing a staining score of 10 (positive cells, 10%; staining intensity, 1+) (×400).

DOI: 10.1309/DT6BJ698LDX2NGGX

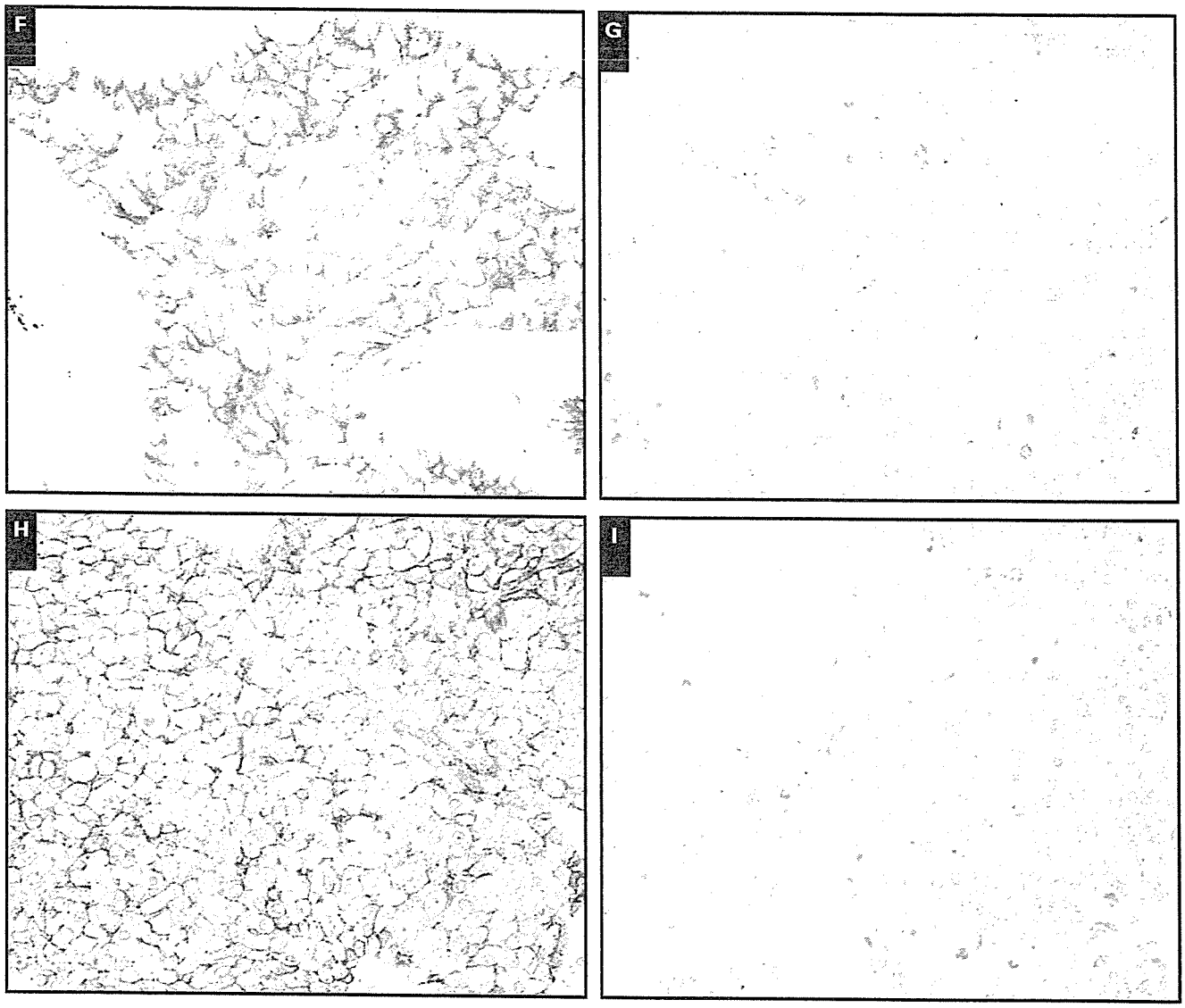

F, CK18 immunostaining of the LCNEC component showing a staining score of 220 (positive cells, 40%; staining intensity, 3+; and positive cells, 50%; staining intensity, 2+) (×400). **G**, CK18 immunostaining of the SCLC component showing a staining score of 10 (positive cells, 10%; staining intensity, 1+) (×400). **H** β-catenin immunostaining of the LCNEC component showing a staining score of 130 (positive cells, 10%; staining intensity, 3+; positive cells, 50%; staining intensity, 2+) (×400). **I**, β-catenin immunostaining of the SCLC component showing a staining score of 20 (positive cells, 20%; staining intensity, 1+) (×400).

However, the staining scores for E-cadherin and β-catenin in LCNEC and SCLC were very different, with both proteins being stained significantly in LCNEC. Moreover, nuclear β-catenin expression was 0% in SCLC, whereas 13% of the LCNEC cases were positive. Because E-cadherin and β-catenin have important roles in the pathogenesis of several human tumors, the E-cadherin cell adhesion system might have different roles in the pathogenesis of some cases of LCNEC.

Of the 3 cases of SCLC combined with LCNEC, 2 showed overexpression of CK7, CK18, and β-catenin in the LCNEC portion, indicating that the results obtained by TMA reliably predicted differences accentuated by morphologic features in these combined tumors. However, no overexpression of these proteins was found in the third case. The reason is unclear; however, the biologic characteristics of LCNEC and SCLC might not have been different despite the morphologic differences in this case.

Sturm and associates[9] reported positive immunostaining for TTF-1 in 85.5% of their SCLC cases and 49% of their LCNEC cases, and the percentage was significantly higher in SCLC. However, in our study, the positive rates and staining scores were lower in SCLC and LCNEC, and TTF-1 was not useful for distinguishing LCNEC from SCLC. Although the cause of the discrepancy is unclear, it has been suggested that

DOI: 10.1309/DT6BJ698LDX2NGGX

the method of selection of the cases, the methods of fixation, or the interpretation of the results might have had a role in these differences.

Improved diagnostic criteria and prospective clinicopathologic studies are needed to validate the impression that patients with LCNEC have a clinical course different from that of patients with SCLC.[22] Our study clearly demonstrated that LCNEC and SCLC have a different biologic phenotype. We conclude that the 4 antibodies identified in our study might be useful for separating LCNEC from SCLC in biopsy specimens that have been crushed or are otherwise difficult to examine morphologically. Further studies are needed to define the expression of these molecules more precisely to enable pathologists to reliably distinguish between LCNEC and SCLC.

From the [1]Pathology Division, National Cancer Center Research Institute East, [2]Thoracic Oncology Division, National Cancer Center Hospital East and, [3]Department of Respiratory Oncology, National Cancer Center Hospital, Chiba, Japan; and [4]First Department of Surgery, Tokyo Medical University, Tokyo, Japan.

Supported in part by Grant-in-Aid for Cancer Research (16-16) from the Ministry of Health, Labour, and Welfare of Japan; by a grant for scientific research expenses for Health Labour and Welfare Programs of Japan; by a grant for Third Term Comprehensive 10-Year Strategy for Cancer Control from the Foundation for the Promotion of Cancer Research; and by Special Coordination Funds for Promoting Science and Technology from the Ministry of Education, Culture, Sports, Science and Technology of the Japanese Government.

Address reprint requests to Dr Ochiai: Pathology Division, National Cancer Center Research Institute East, 6-5-1, Kashiwanoha, Kashiwa-shi, Chiba 277-8577, Japan.

Acknowledgment: We are grateful to Kaoru Hashizume for providing monoclonal antibodies from DakoCytomation.

References

1. Travis WD, Colby TV, Corrin B, et al. *Histological Typing of Lung and Pleural Tumours*. 3rd ed. Heidelberg, Germany: Springer; 1999. *World Health Organization International Histological Classification of Tumours*.
2. Travis WD, Linnoila RI, Tsokos MG, et al. Neuroendocrine tumors of the lung with proposed criteria for large-cell neuroendocrine carcinoma: an ultrastructural, immunohistochemical, and flow cytometric study of 35 cases. *Am J Surg Pathol*. 1991;15:529-553.
3. Hage R, Seldenrijk K, de Bruin P, et al. Pulmonary large-cell neuroendocrine carcinoma (LCNEC). *Eur J Cardiothorac Surg*. 2003;23:457-460.
4. Iyoda A, Hiroshima K, Toyozaki T, et al. Clinical characterization of pulmonary large cell neuroendocrine carcinoma and large cell carcinoma with neuroendocrine morphology. *Cancer*. 2001;91:1992-2000.
5. Paci M, Cavazza A, Annessi V, et al. Large cell neuroendocrine carcinoma of the lung: a 10-year clinicopathologic retrospective study. *Ann Thorac Surg*. 2004;77:1163-1167.
6. Takei H, Asamura H, Maeshima A, et al. Large cell neuroendocrine carcinoma of the lung: a clinicopathologic study of eighty-seven cases. *J Thorac Cardiovasc Surg*. 2002;124:285-292.
7. Travis WD, Rush W, Flieder DB, et al. Survival analysis of 200 pulmonary neuroendocrine tumors with clarification of criteria for atypical carcinoid and its separation from typical carcinoid. *Am J Surg Pathol*. 1998;22:934-944.
8. Demetri G, Elias A, Gershenson D, et al. NCCN Small-Cell Lung Cancer Practice Guidelines. The National Comprehensive Cancer Network. *Oncology (Huntingt)*. 1996;10:179-194.
9. Sturm N, Rossi G, Lantuejoul S, et al. Expression of thyroid transcription factor-1 in the spectrum of neuroendocrine cell lung proliferations with special interest in carcinoids. *Hum Pathol*. 2002;33:175-182.
10. Kononen J, Bubendorf L, Kallioniemi A, et al. Tissue microarrays for high-throughput molecular profiling of tumor specimens. *Nat Med*. 1998;4:844-847.
11. Nocito A, Bubendorf L, Tinner EM, et al. Microarrays of bladder cancer tissue are highly representative of proliferation index and histological grade. *J Pathol*. 2001;194:349-357.
12. Rubin MA, Dunn R, Strawderman M, et al. Tissue microarray sampling strategy for prostate cancer biomarker analysis. *Am J Surg Pathol*. 2002;26:312-319.
13. Hsu SM, Raine L, Fanger H. Use of avidin-biotin-peroxidase complex (ABC) in immunoperoxidase techniques: a comparison between ABC and unlabeled antibody (PAP) procedures. *J Histochem Cytochem*. 1981;29:577-580.
14. Shergill IS, Shergill NK, Araya M, et al. Tissue microarrays: a current medical research tool. *Curr Med Res Opin*. 2004;20:707-712.
15. Lyda MH, Weiss LM. Immunoreactivity for epithelial and neuroendocrine antibodies are useful in the differential diagnosis of lung carcinomas. *Hum Pathol*. 2000;31:980-987.
16. Broers JL, Ramaekers FC, Rot MK, et al. Cytokeratins in different types of human lung cancer as monitored by chain-specific monoclonal antibodies. *Cancer Res*. 1988;48:3221-3229.
17. Chhieng DC, Cangiarella JF, Zakowski MF, et al. Use of thyroid transcription factor 1, PE-10, and cytokeratins 7 and 20 in discriminating between primary lung carcinomas and metastatic lesions in fine-needle aspiration biopsy specimens. *Cancer*. 2001;93:330-336.
18. van de Molengraft FJ, van Niekerk CC, Jap PH, et al. OV-TL 12/30 (keratin 7 antibody) is a marker of glandular differentiation in lung cancer. *Histopathology*. 1993;22:35-38.
19. Wetzels RH, Schaafsma HE, Leigh IM, et al. Laminin and type VII collagen distribution in different types of human lung carcinoma: correlation with expression of keratins 14, 16, 17 and 18. *Histopathology*. 1992;20:295-303.
20. Clavel CE, Nollet F, Berx G, et al. Expression of the E-cadherin–catenin complex in lung neuroendocrine tumours. *J Pathol*. 2001;194:20-26.
21. Rodriguez-Salas N, Palacios J, de Castro J, et al. Beta-catenin expression pattern in small cell lung cancer: correlation with clinical and evolutive features. *Histol Histopathol*. 2001;16:353-358.
22. Marchevsky AM, Gal AA, Shah S, et al. Morphometry confirms the presence of considerable nuclear size overlap between "small cells" and "large cells" in high-grade pulmonary neuroendocrine neoplasms. *Am J Clin Pathol*. 2001;116:466-472.

DOI: 10.1309/DT6BJ698LDX2NGGX

Lung Cancer (2006) 52, 37–45

available at www.sciencedirect.com

SCIENCE DIRECT

journal homepage: www.elsevier.com/locate/lungcan

Differences in clinicopathological and biological features between central-type and peripheral-type squamous cell carcinoma of the lung

Takamoto Saijo[a,b,*], Genichiro Ishii[a], Kanji Nagai[b], Kazuhito Funai[b], Junichi Nitadori[b], Koji Tsuta[a], Michiya Nara[a,b], Tomoyuki Hishida[a,b], Atsushi Ochiai[a]

[a] *Pathology Division, National Cancer Center Research Institute East, Kashiwa, Chiba, Japan*
[b] *Division of Thoracic Oncology, National Cancer Center Hospital East, Kashiwa, Chiba, Japan*

Received 29 September 2005; received in revised form 13 December 2005; accepted 14 December 2005

KEYWORDS
Squamous cell carcinoma;
Peripheral;
Central;
Tissue microarray;
CK 7;
CK 19

Summary The central type and peripheral type squamous cell carcinoma (SCC) of the lung have different clinicopathological characteristics, but, little is known about their biological characteristics. We investigated differences between the properties and phenotypes of peripheral-type (P-type) and central-type (C-type) SCC by performing an immunohistochemical analysis of each type by tissue microarray analysis with a large panel of antibodies. To examine strictly, we selected 20 P-type SCCs that were pathological stage T1 and limited to more peripherally than the fifth bronchial bifurcation, and 21 C-type SCCs that were pathological stage T1 and limited to a lobar bronchus. The results of the clinicopathological study showed that the patients with P-type SCC were significantly older than the patients with C-type SCC and that squamous metaplasia was predominant in C-type SCC than in P-type SCC. The 36 antibodies revealed different expression patterns of cytokeratin 7 (CK 7) and cytokeratin 19 (CK 19) between C-type and P-type SCC. CK 7 expression was more predominant in P-type SCC than in C-type SCC, and CK 19 expression was more predominant in C-type SCC than in P-type SCC. These results suggest that C-type and P-type SCC have different clinicopathological and biological features.

1. Introduction

Squamous cell carcinoma (SCC) accounts for almost 30% of all lung cancers [1,2] and can be classified into a central type (C-type) and a peripheral type (P-type) according to the location of the primary site. A previous report [1] revealed that C-type SCC accounts for two-thirds of all SCCs of the

* Corresponding author at: Division of Thoracic Oncology, National Cancer Center Hospital East, 6-5-1 Kashiwanoha, Kashiwa, Chiba 277-8577, Japan. Tel.: +81 471 33 1111; fax: +81 471 31 4724.
E-mail address: tsaijo@east.ncc.go.jp (T. Saijo).

0169-5002/$ – see front matter © 2006 Elsevier Ireland Ltd. All rights reserved.
doi:10.1016/j.lungcan.2005.12.006

lung, and that the P-type SCC accounts for one-third. C-type SCC has been thought to arise in dysplastic bronchial epithelium through a dysplasia-carcinoma sequence, and this concept of the carcinogenic process is well known as that of uterine cervical neoplasia [3]. However, the carcinogenic process of P-type SCC has never been thoroughly investigated. We recently described different clinicopathologic characteristics of C-type and P-type SCC of the lung. The patients with P-type SCC were significantly older, had lower pathological stage disease, had less lymphatic permeation, and had lymph node metastasis. Only a few previous papers [5,6] have reviewed the clinicopathological characteristics of C-type and/or P-type SCC of the lung. Sakurai et al. reported that small peripheral SCCs have a favorable prognosis. Tanaka et al. reported that P-type SCC of the lung has characteristics similar to adenocarcinoma and originates in glandular epithelium based on the presence of tumor cells that stain PAS-Alb-positive [7,8]. In view of these findings, the carcinogenic pathways of central SCC and peripheral SCC may differ, however, little is known about the biological characteristics of C-type and P-type SCC. In this study, we performed an immunohistochemical analysis of each type of SCC by the tissue microarray technique with a large panel of antibodies to investigate differences between the properties and phenotype of P-type and C-type SCC. Several studies have already proven the feasibility and advantages of the tissue microarray technique and its compatibility with immunohistochemistry on whole-mount sections [9–12]. To strictly identify the location of the sites of C-type and P-type tumors, we first selected SCC cases that were pathological stage T1 (tumor size ≤ 3 cm) and then classified them as the C-type or P-type according to the following definitions: C-type, limited to a lobar bronchus; P-type, limited to more peripherally than the fifth bronchial bifurcation. Below, we report the results of the first study in which tissue microarrays were used to investigate the phenotype of each type (P-type and C-type) of SCC of the lung.

2. Materials and methods

2.1. Case selection

We reviewed about 872 cases of SCC of the lung surgically resected at the National Cancer Center Hospital East between 1992 July and 2004 March. None of them received any preoperative treatment. The tumors were staged according to the International Union Against Cancer's

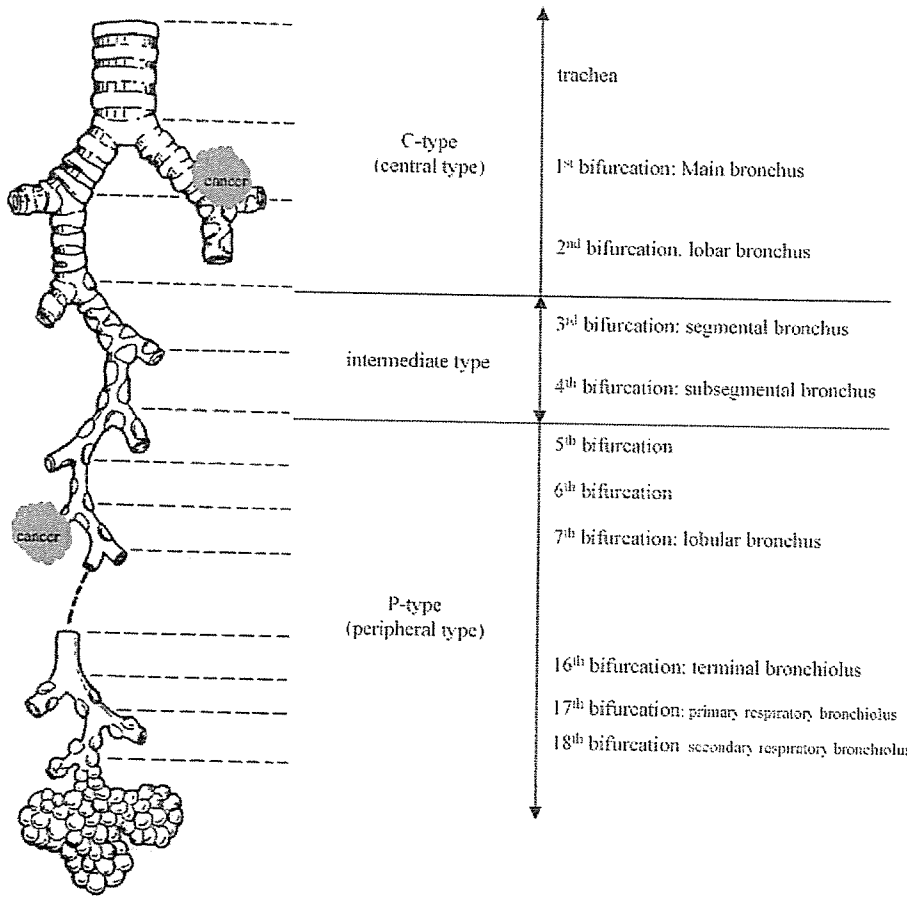

Fig. 1 Definition of squamous cell carcinoma according to location. C-type: limited to the trachea or bronchi; intermediate type: limited to segmental bronchi and subsegmental bronchi; P-type: limited to sites more peripheral than the fifth bronchial bifurcation.

tumor-node-metastasis (TNM) classification and histologically subtyped and graded according to the World Health Organization guidelines. We selected both C-type and P-type cases that were pathological stage T1 (size $\leq$ 3 cm). The evaluation of C-type and P-type was made strictly on the basis of the following criteria: C-type (21 cases), limited to a lobar bronchus; P-type limited to more peripherally than the fifth bronchial bifurcation (Fig. 1). Tumors located in segmental bronchi and subsegmental bronchi were tentatively classified as intermediate type (660 cases) as which were failed to analyze in the present study. We selected 20 cases of P-type SCC and 21 cases of C-type SCC.

2.2. Pathology studies

All samples were stained with van Gieson stain for elastic fibers and PAS-Alb stain for mucin. Vascular involvement and lymphatic permeation was evaluated as positive or negative. Positive for vascular involvement means that extratumoral blood vessel with tumor emboli, and negative for vascular involvement means that intratumoral blood vessel with tumor emboli or no tumor invasion to blood vessel, evaluation for lymphatic permeation is as well. For squamous metaplasia of the bronchus, slides that contained cancer nests were evaluated as positive or negative.

2.3. Microarray construction

The most representative and distinctive tumor areas for each type (P-type and C-type) to be sampled for the TMAs were carefully selected and marked on a hematoxylin-and-eosin-stained slide. The TMAs were assembled with a tissue-arraying instrument (Tissue microprocessor, Tokyo, Japan) consisting of thin-walled stainless steel biopsy needles and stylets used to empty and transfer the needle content. The cylindrical sample was retrieved from the selected region in the donor block and extruded directly into defined array coordinates. Taking tumor heterogeneity into account, we used a large-diameter stylet (2 mm), and the specimens were routinely sampled by taking two core samples of each tumor (different areas). A normal control tissue microarray was used as a positive control for each staining. The slides composed of esophagus, stomach, small intestine, large intestine, liver, pancreas, spleen, brain, heart, lung, skin, testis, kidney, prostate gland, breast, thyroid gland, and adrenal gland. One hundred and forty-four slides 4-μm sections were cut and transferred to slides, deparaffinized with standard xylene, and hydrated through graded alcohols in water. One section from each tissue array block was stained with hematoxylin-and-eosin and covered with a coverslip (Fig. 2). The remaining sections were stored at room temperature for immunohistochemical staining.

2.4. Immunohistochemistry

The antibodies specified in Table 1 were applied to sectioned arrays. Before using them for the arrays, the antibodies were titered against positive control slides, and the concentrations found to provide optimal sensitivity and specificity in the control tissue were used for the TMAs. Antigen

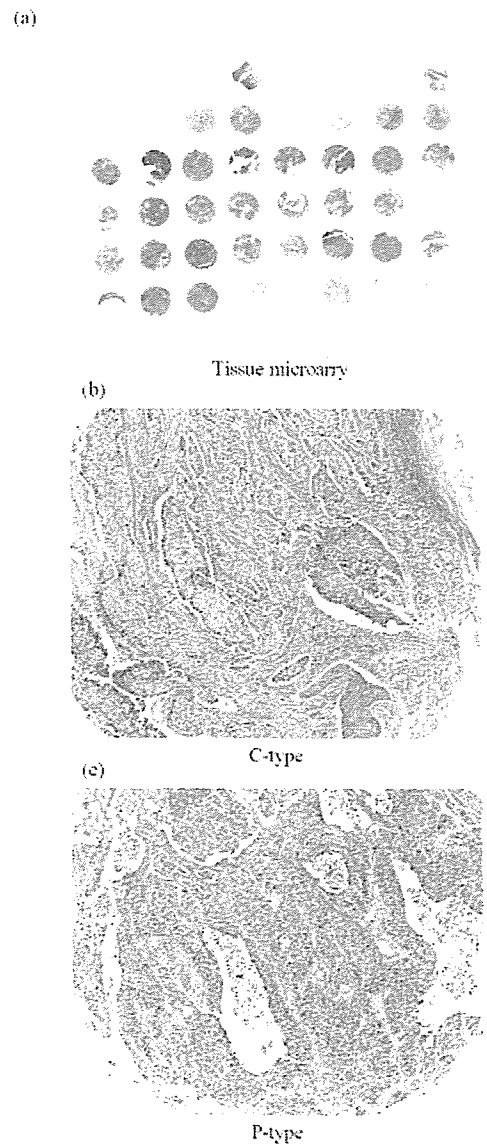

Fig. 2 Tissue microarray slide. (a) Image of a tissue microarray stained with hematoxylin and eosin. The occasional loss of core sections may have been due to failure of the section to adhere to the slide or misalignment of the core in the block. (b) Tissue microarray sections of central-type squamous cell carcinoma stained with hematoxylin and eosin. Bronchial cartilage is shown at the upper right. (c) Tissue microarray sections of peripheral-type squamous cell carcinoma stained with hematoxylin and eosin.

retrieval was performed in citric buffer solution (pH 6.0), except for the slides stained for TTF-1 and P63, which were immersed in the high pH buffer solution (Dako Cytomation). All slides, except the slides stained for CEA, were heated to 95 °C by exposure to microwave irradiation for 20 min. Then, they were allowed to cool for 1 h at room temperature and washed in PBS. Endogenous peroxidase was blocked with 0.3% H_2O_2 in methanol for 15 min, and after incubation overnight with the primary antibodies listed in Table 1 at 4 °C, except the slides stained for TTF-1, 2 days at 4 °C, the

Table 1 List of antibodies

Classification	Antibodies	Clone	Pretreatment	Dilution	Source
Cytokeratins	CK1	34βB4	Microwave	1:20	Novocastra
	CK4	6B14	Microwave	1:100	Novocastra
	CK5/6	D5/16B4	Microwave	1:50	DakoCytomation
	CK7	OV-TL12/30	Microwave	1:50	DakoCytomation
	CK8	35βH11	Microwave	1:25	DakoCytomation
	CK10	DE-K10	Microwave	1:50	DakoCytomation
	CK13	KS-1A3	Microwave	1:100	Novocastra
	CK14	LL002	Microwave	1:20	Novocastra
	CK15	LHK15	Microwave	1:40	Novocastra
	CK17	E3	Microwave	1:20	DakoCytomation
	CK18	DC10	Microwave	1:25	DakoCytomation
	CK19	RCK108	Microwave	1:50	DakoCytomation
	CK20	Ks20.8	Microwave	1:25	DakoCytomation
Apoptosis-associated protain	Bcl-2	124	Microwave	1:40	DakoCytomation
	P53	DO-7	Microwave	1:50	DakoCytomation
Growth factors and hormone receptors	EGFR	EGFR. 113	Microwave	1:10	Novocastra
	C-erbB-2	CB11	Microwave	Prediluted	Ventana Medical Systems
	IGFR	24-31	Microwave	1:100	Chemicon
	C-kit	polyclonal	Microwave	1:50	DakoCytomation
Cell adhesion molecules					
	β-Catenin	14	Microwave	1:200	Becton Dickinson Biosciences
	E-cadherin	36	Microwave	1:100	Becton Dickinson Biosciences
	NCAM	NCC-Lu-243	Microwave	1:25	Nippon Kayaku
	CD44	DF1485	Microwave	1:40	Novocastra
Mucin-related protein	Muc-1	Ma695	Microwave	1:100	Novocastra
	Muc-1 core	Ma552	Microwave	1:100	Novocastra
	Muc-2	Ccp58	Microwave	1:100	Novocastra
	Muc-5AC	CLH2	Microwave	1:50	Novocastra
	Muc-6	CLH5	Microwave	1:50	Novocastra
	M-CCMC-1	HIK1083	Microwave	1:10	Kanto Chemical Co. Inc.
Pneumocyte differential markers	TTF-1	8G7G3/1	Microwave	1:50	DakoCytomation
	SPA	PE-10	Microwave	1:1000	Teijin
	pro-SPC	4A4	Microwave	1:2000	Chemicon
	CEA	CEM010		1:200	Mochida
	CA125	OC125	Microwave	1:200	Japan Turner
	CA19-9	1116NS 19-9	Microwave	1:100	Japan Turner
	P63	7JUL	Microwave	1:50	Dako Cytomation
Proliferation-related protein	Ki-67	MIB-1	Microwave	1:50	Dako Cytomation

slides were incubated with a labeled polymer EnVision TM+, Peroxidase Mouse or Rabbit (Dako, Grostrup, Denmark) for 30 min. The chromogen used was 2% 3,3'-diaminobenzidine in 50 mM Tris-buffer (pH 7.6) containing 0.3% hydrogen. The slides were counterstained with hematoxylin.

2.5. Immunohistochemical scoring and criteria for positive staining

The tissue sections were semiquantitatively scored for membranous and cytoplasmic staining by light microscopy. Labeling scores were determined by multiplying the percentage of positive tumor cells per slide (0–100%) by the predominant level of staining intensity (0 = negative, 1 = weak, 2 = intermediate, 3 = strong). These evaluation methods were used in the previous study using tissue microarray. The scores ranged from 0 to 300, the score for stained two samples were averaged and the result was recorded as score for that case. Specimens that did not stain at all or specimens in which less than 10% of the cells stained were classified as negative. Immunostaining was recorded as positive when more than 10% of the cancer cells exhibited intermediate or strong staining. All samples were evaluated and scored (by T.S. and G.I.) independently without any knowledge of the patients' history. Whenever they disagreed, the slides were reviewed and a consensus was reached.

Table 2 Clinical characteristics of C-type and P-type squamous cell carcinoma

Variables		C-type (21)	P-type (20)	*P*-value
Gender	Male	19	19	0.5782
	Female	2	1	
Age	Mean age	63	69	0.0073*
	Range	49–76	57–76	
Smoking	Non-smoker	0	0	–
	Smoker	21	20	
CEA	5>	13	10	0.4325
	5≤	7	9	
NSE	15>	19	17	–
	15≤	0	0	
SCC	1.5>	20	17	0.2694
	15≤	1	3	

* Considered to be significant ($P<0.05$).

2.6. Statistical analysis

The Stat View statistical software package was used to perform the statistical analyses. The correlations between each type (P-type and C-type) and the clinicopathological variables and results of immunohistochemical staining were evaluated by the χ^2-test or Fisher's exact test, as appropriate. *P*-values <0.05 were considered significant.

3. Results

3.1. Clinical and pathological characteristics of C-type and P-type T1 SCC

Table 2 shows the clinical variables of the patients with each type. The patients with P-type SCC were significantly older

Table 3 Pathological characteristics of C-type and P-type squamous cell carcinoma

Variables		C-type (21)	P-type (20)	*P*-value[a]
Pathological *N* status	pN0	13	17	0.0953
	pN1	8	3	
Lymphatic permeation	Negative	10	11	0.6365
	Positive	11	9	
Vascular involvement	Negative	13	6	0.0406**
	Positive	8	14	
Pleural invasion	Negative	21	15	0.0145**
	Positive	0	5	
Dissemination	Negative	21	20	–
	Positive	0	0	
Pulmonary metastasis	Negative	21	19	0.2995
	Positive	0	1	
Differentiation	Well	1	2	0.8098
	Moderate	9	8	
	Poor	11	10	
Squamous metaplasia of bronchus	Negative	8	15	0.0173**
	Positive	13	5	
Pulmonary fibrosis	Negative	18	17	0.9484
	Positive	3	3	
Emphysema	Negative	18	16	0.6269
	Positive	3	4	

[a] χ^2-test or Fisher's exact test.
** Considered to be significant ($P<0.05$).

than the patients with C-type SCC (mean age: 69 versus 63; $P=0.0073$). Other clinical variables, i.e., gender, smoking status, CEA value, NSE value, and SCC value, were not significantly different.

Table 3 shows the pathological variables of patients with each type. Vascular involvement and pleural invasion were significantly in P-type SCC than in C-type SCC ($P=0.0406$ and $P=0.0145$, respectively). Degree of differentiation did not differ significantly between the two types of SCC. Squamous metaplasia of the bronchus, on the other hand, was observed more frequently in C-type SCC than in P-type SCC ($P=0.0173$).

3.2. Positive rate of the C-type and P-type for each antibody

Of the 3034 cores collected, 359 (12%) were lost during immunohistochemical processing. Table 4 shows the positive staining rates of the C-type SCCs and P-type SCCs for each of the 36 antibodies used in the study. CK 7 immunoreactivity was found in 4.7% of the C-type SCCs and 40.0% of the P-type SCCs, and the difference was significant ($P=0.0047$). A positive reaction for CK 19 was observed in 90.4% of the C-type SCCs, as opposed to 50.0% of the P-type tumors, and the difference was significant ($P=0.0128$). E-cadherin immunoreactivity was observed in 76.1% of the C-type tumors and 45.0% of the P-type tumors, and the difference was significant ($P=0.0407$). Expression of the other cytokeratins, the MUC family, and other types of antigens was insignificant. We also examined about CK 7 and CK 19 immunoreactive expression of metaplasia ($N=18$), which located near C-type (central side metaplasia; $N=10$, 3 was not evaluable) and P-type SCC (peripheral side metaplasia; $N=5$). CK 7 expression showed 7/10 and 4/5 for central and peripheral side meta-

Table 4 Positive rate

	C-type (%)	P-type (%)	P-value[a]
CK-1	4.7	15.0	0.2694
CK-4	9.5	20.0	0.3428
CK-5/6	90.4	85.0	0.9159
CK-7	4.7	40.0	0.0047**
CK-8	71.4	55.0	0.2750
CK-10	28.5	20.0	0.5834
CK-13	47.6	30.0	0.3659
CK-14	28.5	45.0	0.9387
CK-15	23.8	10.0	0.2401
CK-17	66.6	65.0	0.9058
CK-18	76.1	65.0	0.5826
CK-19	90.4	50.0	0.0128**
CK-20	0.0	0.0	–
Bcl-2	4.7	10.0	0.4582
P53	57.1	45.0	0.6555
EGFR	52.3	40.0	0.6211
C-erbB-2	4.7	5.0	0.9108
IGFR	85.7	60	0.0999
C-kit	0.0	5.0	0.2738
β-Catenin	90.4	70.0	0.2732
E-cadherin	76.1	45.0	0.0407**
NCAM	0.0	0.0	–
CD44	71.4	50.0	0.3029
MUC-1	47.6	70.0	0.0929
MUC-1 core	42.8	40.0	0.8527
MUC-2	4.7	0.0	0.3231
MUC-5AC	0.0	0.0	–
MUC-6	0.0	0.0	–
MUC-GGMC-1	0.0	0.0	–
TTF-1	0.0	5.0	0.2995
SPA	0.0	0.0	–
pro-SPC	0.0	0.0	–
CEA	23.8	45.0	0.0892
CA125	0.0	5.0	0.2870
CA19-9	0.0	0.0	–
P63	71.4	65.0	0.9562

[a] χ^2-test.
** Considered to be significant.

Table 5 Scores

	C-type	P-type	P-value[a]
CK-1	2.4 ± 1.2	6.3 ± 3.3	0.2748
CK-4	9.5 ± 5.1	17.8 ± 7.2	0.3543
CK-5/6	206.0 ± 23.7	207.0 ± 23.0	0.9895
CK-7	10.9 ± 7.7	43.2 ± 13.0	0.0354**
CK-8	100.0 ± 12.8	92.0 ± 15.5	0.6918
CK-10	17.0 ± 7.3	6.1 ± 2.9	0.1883
CK-13	56.7 ± 13.1	56.4 ± 21.6	0.9910
CK-14	60.5 ± 19.1	70.0 ± 21.3	0.7407
CK-15	30.0 ± 11.6	11.8 ± 4.7	0.1603
CK-17	63.3 ± 16.6	99.5 ± 18.5	0.1529
CK-18	105.7 ± 16.7	109.2 ± 17.9	0.8869
CK-19	154.3 ± 18.0	87.6 ± 16.9	0.0106**
CK-20	0.2 ± 0.2	0.0 ± 0.0	0.3354
Bcl-2	13.8 ± 6.6	13.6 ± 6.2	0.9828
P53	109.1 ± 21.2	107.5 ± 28.0	0.9645
EGFR	131.0 ± 15.4	134.2 ± 17.7	0.8913
C-erbB-2	6.9 ± 4.0	11.9 ± 10.8	0.6462
IGFR	166.4 ± 15.0	115.0 ±	0.0513
C-kit	1.2 ± 0.7	5.6 ± 5.0	0.3566
β-Catenin	142.0 ± 13.2	108.0 ± 10.4	0.0501
E-cadherin	205.5 ± 15.2	185.3 ± 17.2	0.383
NCAM	0.000 ± 0.0	2.8 ± 2.5	0.2661
CD44	104.5 ± 11.6	109.4 ± 10.5	0.7585
MUC-1	83.3 ± 16.8	93.2 ± 19.7	0.7048
MUC-1 core	44.8 ± 10.7	69.3 ± 16.3	0.2118
MUC-2	10.7 ± 10.7	1.0 ± 0.8	0.3831
MUC-5AC	0.0 ± 0.0	1.0 ± 1.0	0.3115
MUC-6	0.0 ± 0.0	0.0 ± 0.0	–
MUC-GGMC-1	0.0 ± 0.0	0.0 ± 0.0	–
TTF-1	0.0 ± 0.0	9.0 ± 9.0	0.3115
SPA	0.0 ± 0.0	0.0 ± 0.0	–
Pro-SPC	1.0 ± 0.7	5.3 ± 2.2	0.0653
CEA	22.4 ± 8.6	46.8 ± 16.7	0.1894
CA125	1.4 ± 0.9	7.1 ± 3.9	0.1434
CA19-9	2.9 ± 0.9	1.3 ± 0.6	0.1678
P63	132.6 ± 14.2	143.3 ± 19.2	0.6511
Ki-67	296 ± 27/1000	296 ± 25/1000	0.9974

[a] χ^2-test.
** Considered significant.

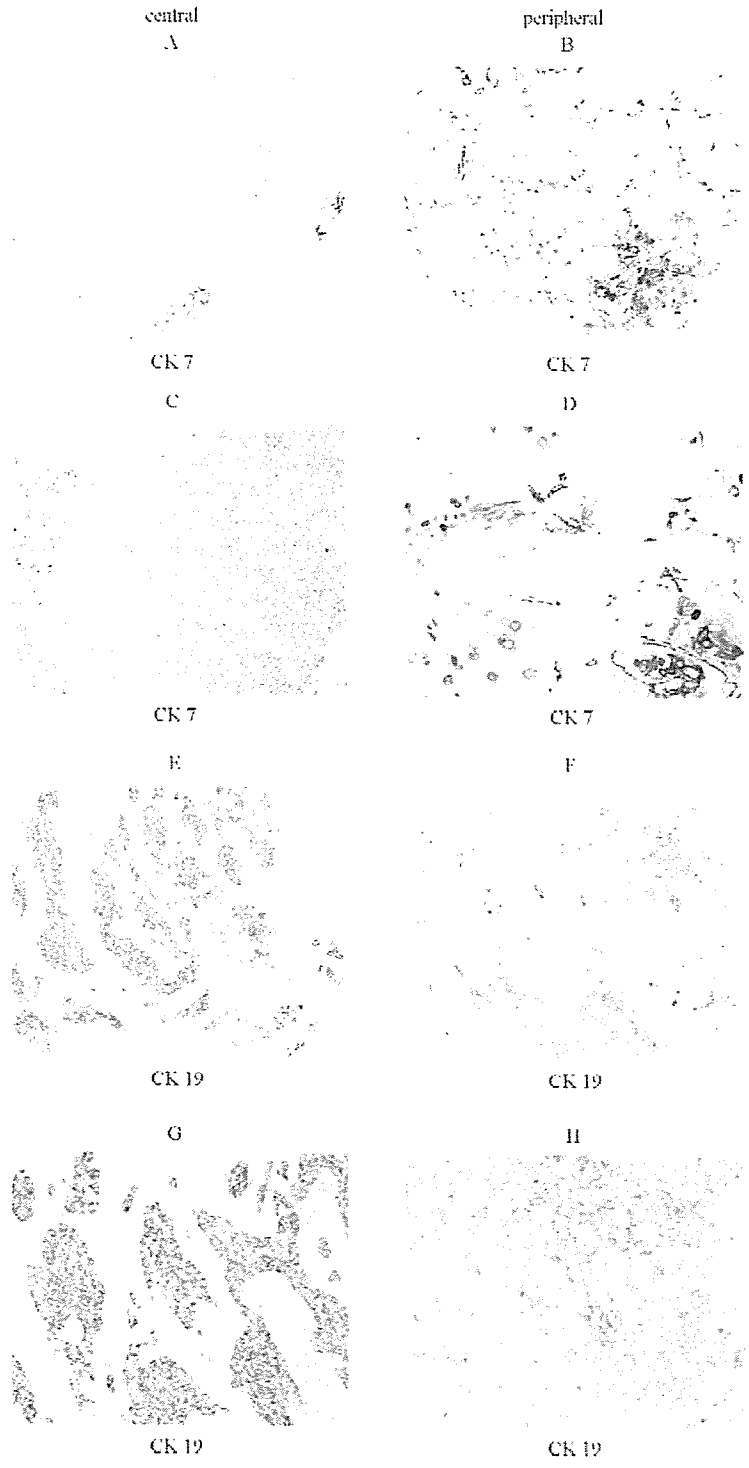

Fig. 3 Immunohistochemical staining of central-type and peripheral-type squamous cell carcinoma. (a) Low magnification (40×) of tissue microarray sections of central-type squamous cell carcinoma stained for CK 7. (b) Low magnification (40×) of tissue microarray sections of peripheral-type squamous cell carcinoma stained for CK 7. (c) High magnification (100×) of tissue microarray sections of central-type squamous cell carcinoma stained for CK 7 (labeling score, 0). (d) High magnification (100×) of tissue microarray sections of peripheral-type squamous cell carcinoma stained for CK 7 (labeling score, $1 \times 40 = 40$). (e) Low magnification (40×) of tissue microarray sections of central-type squamous cell carcinoma stained for CK 19. (f) Low magnification (40×) of tissue microarray sections of peripheral-type squamous cell carcinoma stained for CK 19. (g) Low magnification (100×) of tissue microarray sections of central-type squamous cell carcinoma stained for CK 19 (labeling score, $2 \times 80 = 160$). (h) Low magnification (100×) of tissue microarray sections of peripheral-type squamous cell carcinoma stained for CK 19 (labeling score, $1 \times 80 = 80$).